

Black holes with electroweak hair

Romain Gervalle^{1,*} and Mikhail S. Volkov^{1,†}

¹*Institut Denis Poisson, UMR - CNRS 7013, Université de Tours, Parc de Grandmont, 37200 Tours, France*

We construct static and axially symmetric magnetically charged hairy black holes in the gravity-coupled Weinberg-Salam theory. Large black holes merge with the Reissner-Nordström (RN) family, while the small ones are extremal and support a hair in the form of a ring-shaped electroweak condensate carrying superconducting W-currents and up to 22% of the total magnetic charge. The extremal solutions are asymptotically RN with a mass *below* the total charge, $M < |Q|$, due to the negative Zeeman energy of the condensate interacting with the black hole magnetic field. Therefore, they cannot decay into RN black holes. As their charge increases, they show a phase transition when the horizon symmetry changes from spherical to oblate. At this point they have the mass typical for planetary size black holes of which $\approx 11\%$ are stored in the hair. Being obtained within a well-tested theory, our solutions are expected to be physically relevant.

In 1971 Ruffini and Wheeler formulated the no-hair conjecture according to which the only parameters of an isolated black hole should be its mass, angular momentum, and electric/magnetic charge [1]. The conjecture was supported by the no-hair theorems proven for a number of special cases (see, e.g., [2, 3]). The first counter-example was discovered in 1989: static black holes with a non-trivial Yang-Mills field but without a charge [4]. This finding was generalized in many ways leading to a plethora of black holes supporting a Skyrme hair [5], a Higgs hair [6, 7], stringy hair [8], hair without spherical symmetry [9], and many others; see [10] for a review. More recently were discovered hairy black holes in the Horndeski theory [11], black holes supporting “spinning clouds” of ultra-light bosons [12], black holes with a massive graviton hair [13], etc. [14, 15].

Nowadays hairy black holes have become a commonplace, but one may wonder if they really exist in Nature? Unfortunately, all known solutions were obtained within either simplified models or exotic models relying on the existence of yet undiscovered particles and fields. Therefore, their physical relevance is not immediately obvious. To be relevant, a solution should be obtained within a well-tested physical theory, which is the Standard Model (SM) of fundamental interactions coupled to the General Relativity (GR). The former contains the QCD sector where quantum effects are dominant, but in the electroweak (EW) sector the quantum corrections are not too large. Therefore, it makes sense to study extended classical configurations in the Einstein-Weinberg-Salam (EWS) theory. This theory contains the electrovacuum sector with the Kerr-Newman black holes, but does it allow for some other black holes as well?

In fact, such solutions do exist but are difficult to construct since magnetically charged hairy EW black holes are not spherically symmetric, unless in an unphysical limit of the theory [7], or for the low value of the magnetic charge [16]. Non-spherical black holes were considered perturbatively in theories which are similar to the

EWS but without the Z boson [17], or without both Z and Higgs bosons [18]. A fully non-perturbative analysis within the EWS theory has been missing up to now.

Maldacena has qualitatively described such black holes [19]. They are not spherically symmetric because a very strong magnetic field creates the EW condensate of vortices [20–23] forming a “corona” around the black hole. This happens in the region where the hypermagnetic field B falls within the interval $m_{\text{H}}^2 > B > m_{\text{W}}^2$. If $B > m_{\text{H}}^2$ at the horizon, then the black hole is surrounded in addition by a bubble of symmetric phase. In the far field all massive fields assume vacuum values and the magnetic field becomes spherically symmetric.

Following this scenario, various aspects of magnetic black holes have been discussed, but always at the qualitative level [24–28]. Therefore, in what follows we confirm the scenario by explicitly constructing the solutions in the special case of axial symmetry when the EW condensate reduces to rings around the equatorial plane. Analyzing the general case would require 3D simulations. We sketch below only essential points and systematically refer to the Supplemental Materials [29] for details; an extended version will be presented separately [30].

The theory. We consider the bosonic part of the EWS theory containing gravity described by the metric $g_{\mu\nu}$, a complex doublet Higgs field Φ , a U(1) hypercharge field $B = B_{\mu}dx^{\mu}$, and an SU(2) field $W = T_a W_{\mu}^a dx^{\mu}$ with $T_a = \tau_a/2$ where τ_a are Pauli matrices. The action is

$$\mathcal{S} = \frac{e^2}{4\pi\alpha} \int \left(\frac{1}{2\kappa} R - \frac{1}{4g^2} W_{\mu\nu}^a W^{a\mu\nu} - \frac{1}{4g'^2} B_{\mu\nu} B^{\mu\nu} - (D_{\nu}\Phi)^{\dagger} D^{\nu}\Phi - \frac{\beta}{8} (\Phi^{\dagger}\Phi - 1)^2 \right) \sqrt{-g} d^4x. \quad (1)$$

Here R is the Ricci scalar, $B_{\mu\nu} = \partial_{\mu}B_{\nu} - \partial_{\nu}B_{\mu}$ and $W_{\mu\nu}^a = \partial_{\mu}W_{\nu}^a - \partial_{\nu}W_{\mu}^a + \epsilon_{abc}W_{\mu}^b W_{\nu}^c$ are the U(1) and SU(2) gauge field strengths, the Higgs covariant derivative is $D_{\mu}\Phi = (\partial_{\mu} - \frac{i}{2}B_{\mu} - \frac{i}{2}\tau_a W_{\mu}^a)\Phi$, and the Higgs self-coupling is $\beta \approx 1.88$. The two coupling constants $g = \cos\theta_{\text{W}}$ and $g' = \sin\theta_{\text{W}} \approx \sqrt{0.22}$ determine the electron charge $e = gg'$ and $\alpha \approx 1/137$ is the fine structure constant. Everything is dimensionless, the Z, W, and Higgs masses are $m_{\text{Z}} = 1/\sqrt{2}$, $m_{\text{W}} = gm_{\text{Z}}$, $m_{\text{H}} = \sqrt{\beta}m_{\text{Z}}$

* romain.gervalle@univ-tours.fr

† mvolkov@univ-tours.fr

in units of the mass scale 128.9 GeV, whose Compton wavelength 1.53×10^{-16} cm sets the length scale. The gravity coupling is $\kappa = (4e^2/\alpha)(m_z/M_{\text{Pl}})^2 = 5.42 \times 10^{-33}$ where M_{Pl} is the Planck mass [29].

The electromagnetic field is $e\mathcal{F}_{\mu\nu} = g^2 B_{\mu\nu} - g'^2 n_a W_{\mu\nu}^a$ with $n_a = (\Phi^\dagger \tau_a \Phi)/(\Phi^\dagger \Phi)$, the current $4\pi \mathcal{J}^\mu = \nabla_\nu \mathcal{F}^{\mu\nu}$ [31]. The dual tensor $\tilde{\mathcal{F}}^{\mu\nu}$ defines the magnetic field $\mathcal{B}^k = \tilde{\mathcal{F}}^{0k}$ and the magnetic charge density $4\pi \tilde{\mathcal{J}}^0 = \nabla_k \mathcal{B}^k$. The hypermagnetic field is $B^k = \tilde{B}^{0k}$. The closed part of $\mathcal{F}_{\mu\nu}$ defines similarly a neutral current J^μ [29].

Abelian solutions. Varying the action gives the field equations [29], whose simplest solution corresponds to a vacuum geometry with $B = W = 0$ and $\Phi^{\text{tr}} = (0, 1)$. Choosing the gauge fields within the Cartan subalgebra, gives the *Abelian* solution with the RN geometry,

$$ds^2 = -N(r) dt^2 + \frac{dr^2}{N(r)} + r^2(d\vartheta^2 + \sin^2 \vartheta d\varphi^2), \quad (2)$$

$$B = -(n/2) \cos \vartheta d\varphi, \quad W = T_3 B, \quad \Phi^{\text{tr}} = (0, 1),$$

with $N(r) = 1 - 2M/r + Q^2/r^2$ and $Q^2 = (\kappa/2) P^2$ where $P = n/(2e)$ and $n \in \mathbb{Z}$. The gauge fields show the Dirac string singularity at $\vartheta = 0, \pi$, which can be removed by gauge transformations. The radial hypermagnetic field is $B = n/(2r^2)$ while the magnetic field $\mathcal{B} = P/r^2 = B/e$ corresponds to the Dirac monopole. The solution (2) describes the magnetic RN black hole of charge P . The event horizon is at $r_h = M + \sqrt{M^2 - Q^2}$.

Another simple solution is obtained by setting in (2) $W = \Phi = 0$ while keeping the same B and choosing $N(r) = 1 - 2M/r + g^2 Q^2/r^2 - (\Lambda/3) r^2$ with $\Lambda = \kappa\beta/8$. This time the magnetic field is $\mathcal{B} = g^2 P/r^2 = g^2 B/e$ hence the solution describes the RN-de Sitter (RNdS) black hole of charge $g^2 P$. In the extremal limit the two black hole horizons merge, then

$$N(r) = \left(1 - \frac{r_{\text{ex}}}{r}\right)^2 \left(1 - \frac{\Lambda}{3} [r^2 + 2rr_{\text{ex}} + 3r_{\text{ex}}^2]\right), \quad (3)$$

where $1 - 2\Lambda r_{\text{ex}}^2 = \sqrt{1 - Q^2/Q_m^2}$ with $Q_m = 1/(2g\sqrt{\Lambda})$.

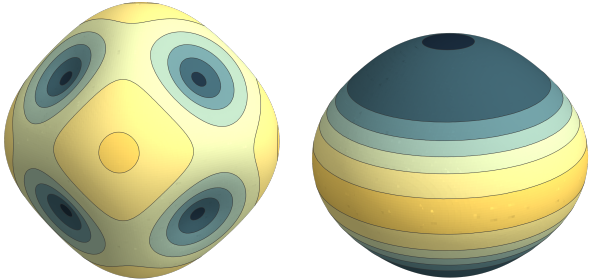


Figure 1. Left: the horizon distribution of the W-condensate $\bar{w}^\mu w_\mu$ minimizing the energy for $n = 10$. The level lines coincide with the current flow forming loops around radial vortex pieces (dark spots). The condensate and vortex fields are maximal in the yellow regions. Right: the same when all vortices merge into two oppositely directed multi-vortices.

Perturbative analysis. Perturbing all fields around the RN solution (2) and linearizing with respect to perturbations, the field $w_\mu = (\delta W_\mu^1 + i\delta W_\mu^2)/g$ decouples from the rest (in the unitary gauge) and fulfills the equations admitting the following solution [29]:

$$w_\mu dx^\mu = e^{i\omega t} \psi(r) (\sin \vartheta)^{j+1} \sum_{m \in [-j, j]} c_m z^{m-1} dz. \quad (4)$$

Here $j = |n|/2 - 1$ is the orbital angular momentum, $|n| > 1$ (if $|n| = 1$ then w_μ is unbounded at $\vartheta = 0, \pi$), $z = \tan(\vartheta/2) \exp(-in\varphi/|n|)$, while c_m are arbitrary coefficients. The function $\psi(r)$ fulfills the equation

$$\left(-\frac{d^2}{dr_*^2} + N(r) \left[m_w^2 - \frac{|n|}{2r^2}\right]\right) \psi(r) = \omega^2 \psi(r), \quad (5)$$

with $dr_* = dr/N(r)$. If $N(r) = 1$, this equation always admits normalizable solutions with $\omega^2 < 0$, hence Dirac monopoles in flat space are always unstable with respect to the formation of a W-condensate [32]. If $N(r)$ corresponds to the RN solution, the instability is absent for a large horizon radius r_h , but settles in for $r_h = r_h^0(n)$ when the equation admits a solution with $\omega = 0$ describing a static deformation of the black hole by a condensate. Therefore, r_h^0 is the bifurcation point where the first hairy black hole solutions deviate from the RN family.

Solving Eq.(5) numerically yields $r_h^0(n) = 0.89, 2.68, 10.29$ for $n = 2, 10, 100$, respectively. For $|n| \gg 1$ one has $r_h^0(n) \approx 1.13 \sqrt{|n|} = \sqrt{|n|}/g$ hence $B(r_h^0) \approx m_w^2$. If $|n| = 2$ then $j = 0$ and the hair is spherically symmetric, but if $|n| > 2$ then $j > 0$ and the hair is not spherical.

The coefficients c_m are fixed by going to higher orders of perturbation theory and minimizing the condensate energy [29]. This gives the result shown in Fig.1 (left): a ‘‘platonic’’ distribution of radial vortex pieces forming the corona. The vortices extend along the radial direction and are encircled by loops of current $J_\nu = e\Im[\nabla^\sigma(w_\sigma \bar{w}_\nu)]$ tangent to the horizon. According to the EW anti-Lenz law [20–23], the vortex fields vanish at the vortex center where the condensate vanishes and become maximal where the condensate is maximal.

The choice $c_m = \delta_{m0}$ is also a critical point of the energy, although not the global minimum. It corresponds to the axially symmetric configuration in which all vortices merge into two oppositely directed multi-vortices supported by azimuthal currents; see Fig.1 (right).

Summarizing, the perturbative analysis shows zero modes describing the hair that starts to grow. The hairy solutions are not spherically symmetric for $|n| > 2$, but they can be axially symmetric, and these we are able to construct also at the non-perturbative level.

Axial symmetry. We choose the fields as follows,

$$ds^2 = -e^{2U} N(r) dt^2 + e^{-2U} dl^2, \quad (6)$$

$$dl^2 = e^{2K} \left[\frac{dr^2}{N(r)} + r^2 d\vartheta^2 \right] + e^{2S} r^2 \sin^2 \vartheta d\varphi^2,$$

$$W = T_2 (F_1 dx + F_2 d\vartheta) - \frac{n}{2} (T_3 F_3 - T_1 F_4) d\varphi,$$

$$B = -(n/2) Y d\varphi, \quad \Phi^{\text{tr}} = (\phi_1, \phi_2).$$

Here $U, K, S, F_1, F_2, F_3, F_4, Y, \phi_1, \phi_2$ are 10 real functions of r, ϑ subject to certain boundary conditions [29]. The gauge fields W, B show the Dirac string singularity that can be gauged away if $n \in \mathbb{Z}$ [29]. They also have a residual $U(1)$ gauge invariance that can be fixed by imposing a gauge condition [29]. The radial coordinate r (not the same as the Schwarzschild coordinate r) is defined up to reparametrizations, its choice is specified by fixing the auxiliary function $N(r)$. For non-extremal solutions we set $N(r) = 1 - r_H/r$ where the black hole “size” r_H does not have a direct physical meaning but labels the solutions. We obtain solutions for the 10 functions in (6) for values of the gravity coupling $10^{-10} < \kappa < 10^{-2}$ and then extrapolate to the physical value $\kappa \sim 10^{-33}$. We use the FreeFem numerical solver [33].

Hairy black holes. They have the same charge as in the RN case, $P = n/(2e)$. Choosing a value $|n| > 2$ (such that $Q = \sqrt{\kappa/2}P \ll Q_m$) determines the size $r_H = r_H^0(n)$ for which the RN solution starts to develop a hair [29]. Next, we decrease the size r_H and the horizon shrinks, but the massive hair grows longer spanning the interval $r \in [r_H, r_H^0]$. When r_H descends below a certain value r_H^b such that $B(r_H^b) \approx m_w^2$, the massive hair does not grow anymore and rests confined in the region $r_H^b < r < r_H^0$ where $m_w^2 > B > m_w^2$. In the near-horizon region, $r_H < r < r_H^b$, the hypermagnetic field becomes too strong, $B > m_w^2$, driving to zero W and Φ and creating a bubble of symmetric phase around the horizon (see Fig.2). The bubble expands as r_H decreases further, and in the $r_H \rightarrow 0$ limit the horizon surface gravity approaches zero but the horizon area remains finite.

Using the magnetic current density defined above, one can compute the charge contained in the hair, $P_h = \int_{r>r_H} \tilde{J}^0 \sqrt{-g} d^3x$, while the rest $P_H = P - P_h$ is inside the black hole. Defining $\lambda = P_h/P$, we observe that $\lambda \rightarrow 0$ at the bifurcation point while in the extremal limit one has $\lambda \rightarrow g'^2$ hence $P_h = g'^2 P = 0.22 \times P$ (see Fig.3).

Summarizing, hairy black holes exist for $r_H \in [0, r_H^0]$. They loose hair in the RN limit $r_H \rightarrow r_H^0$ when all the charge is inside the black hole, and they become maximally hairy in the extremal limit $r_H \rightarrow 0$ when 22% of the magnetic charge moves to the hair.

The ADM mass M is determined from the asymptotic

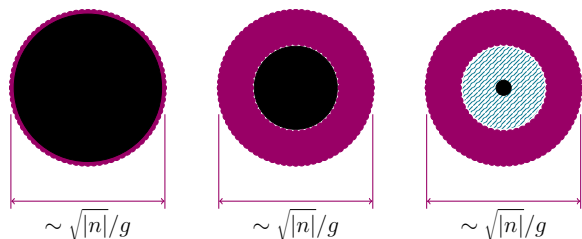


Figure 2. When the horizon size decreases, the massive hair emerges (left), grows longer (center), then a bubble of symmetric phase appears around the horizon (right).

expansion $g_{00} = -1 + 2M/r + \mathcal{O}(1/r^2)$ or from the formula

$$M = \frac{k_H A_H}{4\pi} + \frac{\kappa}{8\pi} \int_{r>r_H} (-T^0_0 + T^k_k) \sqrt{-g} d^3x. \quad (7)$$

Here $k_H = (1/2) N' e^{2U-K} |_{r=r_H}$ is the surface gravity and $A_H = 2\pi r_H^2 \int_0^\pi e^{K+S-2U} \sin \vartheta d\vartheta |_{r=r_H}$ is the horizon area. The total mass splits as $M = M_H + M_h$ where the horizon contribution M_H is defined as the mass of the RN black hole with the same area A_H and with the charge P_H [29]. The mass M decreases with decreasing r_H and, unless $|n|$ is very large, one always has $M \approx M_H$. The relative contribution of the hair mass M_h/M_H grows with n , it is maximal in the extremal limit and vanishes in the RN limit (see Fig.3).

We define the horizon radius as $r_h = \sqrt{A_H/(4\pi)}$, but since the horizon is non-spherical, one should define also the equatorial radius $r_h^{eq} = \sqrt{g_{\varphi\varphi}(r_H, \pi/2)}$ and the polar radius $r_h^{pl} = (1/\pi) \int_0^\pi \sqrt{g_{\vartheta\vartheta}(r_H, \vartheta)} d\vartheta$, which determine the horizon oblateness $\delta = r_h^{eq}/r_h^{pl} - 1$.

Far away from the horizon the massive fields decay and the theory reduces to electrovacuum, hence one can define [29] the gravitational Q_G and magnetic Q_M quadrupole moments following the approach of [34–37]. As seen in Fig.3, the quadrupole moments grow as r_H decreases, reaching maximal values in the extremal limit. The horizon oblateness δ also grows at first but then decreases and vanishes in the extremal limit, when the horizon geometry becomes perfectly spherical, although the hair is oblate.

Extremal solutions. They have zero surface gravity. The value of their charge $Q_* \approx 0.6 Q_m$ with $Q_m = 1/(2g\sqrt{\Lambda})$ separates two phases, with the horizon oblateness δ being the order parameter.

Phase I: $|Q| < Q_*$, $\delta = 0$. The solutions interpolate between the extremal RNdS described by Eq.(3) at the horizon and the RN given by Eq.(2) in the asymptotic region. We obtain them by choosing the auxiliary metric function $N(r) \propto (1 - r_{ex}/r)^2$ [29]. The horizon radius is $r_{ex} = g|Q| + \mathcal{O}(|n|^3 \kappa^{5/2})$ and the area $A_H = 4\pi r_{ex}^2$.

The configurations harbour at the center a small black hole containing 78% of the total magnetic charge and sup-

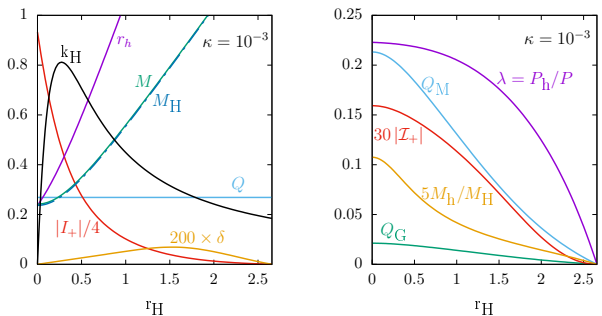


Figure 3. Parameters of non-extremal solutions with $n = 10$, $\kappa = 10^{-3}$. For $r_H \rightarrow 0$ they become extremal, for $r_H \rightarrow 2.5$ they loose hair and become RN.

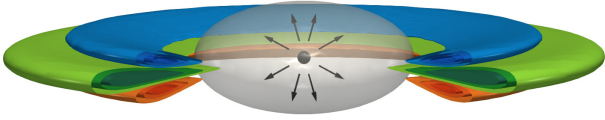


Figure 4. The extremal solutions contain a small charged black hole inside a bubble of symmetric phase, surrounded by a ring-shaped EW condensate supporting 22% of the total magnetic charge and two opposite superconducting W-currents. These create pieces of two magnetic multi-vortices along the positive and negative z -directions. Farther away the condensate disappears and the magnetic field becomes radial.

porting a strong B-field which creates a bubble of symmetric phase where $W \approx \Phi \approx 0$. The bubble spans the region of size $r_b \approx \sqrt{|n|/\beta} \approx 0.73\sqrt{|n|}$ where $B > m_H^2$. Farther away, where $m_H^2 > B > m_W^2$, the massive fields deviate from zero and form a ring-shaped condensate, as shown in Fig.4. The central ring (green online) contains the remaining 22% of the charge whose distribution is described by the magnetic charge density \tilde{J}^0 . This ring is sandwiched between two others (blue and red online) containing equal but oppositely directed superconducting currents \mathcal{I}_+ and \mathcal{I}_- (in units of 1.4×10^8 A) due to fluxes of \mathcal{J}^φ in the upper and lower half-spaces. Fluxes of J^φ , I_\pm , look similarly but have a much larger amplitude.

The condensate terminates where $B \approx m_W^2$, at $r_c \approx \sqrt{|n|/g} \approx 1.13\sqrt{|n|}$, which determines the corona size. Still farther away the configuration approaches the RN solution (2) whose mass is *less* than the charge,

$$M < |Q|. \quad (8)$$

This is because, although the hair carries the charge $Q_h = 0.22 \times Q$, its mass M_h is small due to the negative Zeeman energy of the condensate interacting with the magnetic field of the black hole, which shifts the W-mass as $m_W^2 \rightarrow m_W^2 - |B|$ [21]. As a result, the mass-to-charge ratio for the hair is small, $M_h/|Q_h| \sim \sqrt{\kappa} \ll 1$, which can be viewed as a manifestation of the weak gravity conjecture [38]. The condensate is magnetically repelled by the black hole stronger than attracted gravitationally, but it cannot fly away because it has to obey the Yukawa law. Since the hair mass is small, one has $M = M_H + M_h \approx M_H = (r_{\text{ex}} + g^2 Q^2 / r_{\text{ex}}) / 2 \approx g|Q| < |Q|$.

Extrapolating our results to the physical value $\kappa \sim 10^{-33}$ yields the following picture. The horizon size $r_{\text{ex}} \propto Q \propto \sqrt{\kappa}$ is *parametrically* small as compared to the size of the hairy region $\sim \sqrt{|n|}$. Therefore, the tiny black hole does not affect the electroweak hair but only creates the B-field accounting for the horizon part of the mass, $M_H = g|Q| \propto \sqrt{\kappa}$. The hair carries the mass $M_h \sim \kappa$ and lives far away from the horizon, in the region where the geometry is almost flat. The total mass in units of the electroweak mass scale is $e^2/(4\pi\alpha) \times \mathcal{M}$, where [29]

$$\mathcal{M} \equiv \frac{8\pi}{\kappa} \times M = \frac{4\pi g|n|}{\sqrt{2\kappa}e} + \frac{8\pi}{\kappa} M_h \equiv \mathcal{M}_H + \mathcal{M}_h. \quad (9)$$

The horizon contribution \mathcal{M}_H corresponds to the mass $5.1|n| M_{\text{Pl}}$ which diverges in the $\kappa \rightarrow 0$ limit, but the hair contribution \mathcal{M}_h remains finite and reduces precisely to the regularized mass of the flat space EW monopoles: the Cho-Maison monopole [39] for $n = 2$ and its generalizations for $n > 2$ [40]. As a result, extremal solutions can be viewed as flat space monopoles harbouring in the center a tiny RNdS black hole which almost does not affect the EW fields. The total mass of flat space EW monopoles is infinite, hence it costs infinite energy to create them, but gravity renders the mass finite due to the cutoff at the horizon. Therefore, the extremal black holes provide the ‘‘classical UV completion’’ for the EW monopoles.

When increasing the charge $Q \propto |n|$, the bubble size and hair length scale as $\sqrt{|Q|}$, but the horizon size $r_{\text{ex}} \propto |Q|$ grows faster and the black hole absorbs the bubble. The hair mass M_h grows faster than the horizon mass M_H increasing the ratio $M/|Q|$. The horizon value of the B-field is $\propto Q/r_{\text{ex}}^2 \propto 1/Q$, hence it *decreases*, and when $B < m_H^2$, the Higgs field deviates from zero at the horizon, the bubble is totally absorbed and the solution enters next phase.

Phase II: $|Q| > Q_*$, $\delta > 0$. The horizon geometry changes from spherical to oblate and is no longer described by the extremal RNdS solution (3) [29]. One has $\delta \propto (|Q| - Q_*)^s$ at the transition point, which resembles a second order phase transition (the critical exponent is rather large, $s \approx 10.8$ if $\kappa = 10^{-2}$). In addition, the fraction of the hair charge which was constant in the previous phase, $\lambda = P_h/P = 0.22$, starts to decrease (see Fig.5). The black hole absorbs the corona and becomes less hairy, the ratio $M/|Q|$ increases, the geometry approaches the extremal RN and finally merges with it when the horizon size overtakes the corona size, then $|Q| = r_h^0(n) = \sqrt{|n|/g}$. This corresponds to the maximal charge $Q_{\text{max}} = 2g'\sqrt{\beta} Q_m = 1.29 Q_m$. No hairy solutions exist beyond this value of charge.

The black hole is maximally hairy for $Q \approx Q_*$ ($|n| \approx 1.5 \times 10^{32}$) when the ratio M_h/M is maximal (see Fig.5). Then the horizon size is ≈ 3 cm and the total mass $\approx 2 \times 10^{25}$ kg is typical for the planetary mass black holes, of which $\approx 11\%$ (if $\kappa = 10^{-2}$) is stored in the hair.

Summary. We obtain the hairy solutions within the

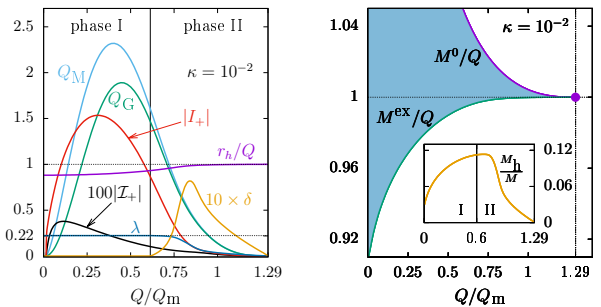


Figure 5. The parameters of extremal solutions (left) and the existence diagram for hairy solutions (right) for $\kappa = 10^{-2}$.

region corresponding to the shaded area in Fig.5 (right panel): below the upper curve corresponding to the bifurcation with the RN branch and above the lower curve corresponding to the extremal solutions. Solutions for $|n| > 2$ are new. The corona greatly enhances the evaporation rate [19], hence non-extremal holes should quickly relax to the extremal state where $M \leq |Q|$, therefore they cannot decay into RN black holes.

However, they can still lower their energy by developing a “hedgehog” of radial vortices forming the corona. In the axially-symmetric case the corona degenerates into two oppositely directed multi-vortices, unstable due to the repulsion between the elementary vortices. Therefore, the axially symmetric corona is expected to split into elementary vortices with maximal mutual separations, similarly to what is shown in Fig.1. Such “platonic” black holes should be classically stable, but describing them non-perturbative solutions are not yet known.

Since they are described by well-tested theories, the

hairy EW black holes are expected to be physically relevant. They could probably originate from primordial black holes. Suppose that the fluctuating hypermagnetic field in the ambient EW plasma becomes at some moment mostly orthogonal to the black hole horizon, or that a piece of a magnetic vortex gets attached to the horizon. This will create a flux through the horizon, hence a charge, to be compensated by the opposite flux created on other black hole(s). The oppositely charged black holes will not necessarily annihilate, being pushed apart by the cosmic expansion, or maybe they form bound systems stabilized by a scalar repulsion [41]. Such a mechanism for the charge generation should be verified, but if true, it would imply that no new physics beyond the SM is needed for monopoles. Therefore, the extremal hairy EW black holes are the plausible candidates for magnetic monopoles which may perhaps exist in Nature.

Acknowledgements. We thank Eugen Radu, Maxim Chernodub and Julien Garaud for discussions.

-
- [1] R. Ruffini and J. Wheeler, *Phys.Today* **24**, 30 (1971), 1206.3482.
- [2] J. D. Bekenstein, *Phys. Rev. D* **5**, 1239 (1972).
- [3] A. Saa, *J. Math. Phys.* **37**, 2346 (1996), arXiv:gr-qc/9601021.
- [4] M. S. Volkov and D. V. Galtsov, *JETP Lett.* **50**, 346 (1989), [*Pisma Zh. Eksp. Teor. Fiz.*50,312(1989)].
- [5] S. Droz, M. Heusler, and N. Straumann, *Phys. Lett. B* **268**, 371 (1991).
- [6] P. Breitenlohner, P. Forgács, and D. Maison, *Nucl. Phys. B* **383**, 357 (1992).
- [7] B. R. Greene, S. D. Mathur, and C. M. O’Neill, *Phys. Rev. D* **47**, 2242 (1993), arXiv:hep-th/9211007.
- [8] P. Kanti, N. E. Mavromatos, J. Rizos, K. Tamvakis, and E. Winstanley, *Phys. Rev. D* **54**, 5049 (1996), arXiv:hep-th/9511071.
- [9] B. Kleihaus and J. Kunz, *Phys. Rev. Lett.* **79**, 1595 (1997).
- [10] M. S. Volkov and D. V. Gal’tsov, *Phys. Rept.* **319**, 1 (1999), arXiv:hep-th/9810070 [hep-th].
- [11] T. P. Sotiriou and S.-Y. Zhou, *Phys. Rev. D* **90**, 124063 (2014).
- [12] C. A. R. Herdeiro and E. Radu, *Phys. Rev. Lett.* **112**, 221101 (2014), arXiv:1403.2757 [gr-qc].
- [13] R. Gervalle and M. S. Volkov, *Phys. Rev. D* **102**, 124040 (2020), arXiv:2008.13573 [hep-th].
- [14] C. A. R. Herdeiro and E. Radu, *Int. J. Mod. Phys. D* **24**, 1542014 (2015), arXiv:1504.08209 [gr-qc].
- [15] M. S. Volkov, (2016), arXiv:1601.08230 [gr-qc].
- [16] Y. Bai and M. Korwar, *JHEP* **04**, 119 (2021), arXiv:2012.15430 [hep-ph].
- [17] K.-M. Lee and E. J. Weinberg, *Phys. Rev. Lett.* **73**, 1203 (1994), arXiv:hep-th/9406021.
- [18] S. A. Ridgway and E. J. Weinberg, *Phys. Rev. D* **52**, 3440 (1995), arXiv:gr-qc/9503035.
- [19] J. Maldacena, *JHEP* **04**, 079 (2021), arXiv:2004.06084 [hep-th].
- [20] J. Ambjorn and P. Olesen, *Nucl. Phys. B* **315**, 606 (1989).
- [21] J. Ambjorn and P. Olesen, *Int. J. Mod. Phys. A* **5**, 4525 (1990).
- [22] M. N. Chernodub, J. Van Doorselaere, and H. Verschelde, *Phys. Rev. D* **88**, 065006 (2013), arXiv:1203.5963 [hep-ph].
- [23] M. N. Chernodub, V. A. Goy, and A. V. Molochkov, *Phys. Rev. Lett.* **130**, 111802 (2023), arXiv:2206.14008 [hep-lat].
- [24] Y. Bai, J. Berger, M. Korwar, and N. Orlofsky, *JHEP* **10**, 210 (2020), arXiv:2007.03703 [hep-ph].
- [25] Y. Bai, S. Lu, and N. Orlofsky, *Phys. Rev. Lett.* **127**, 101801 (2021), arXiv:2103.06286 [hep-ph].
- [26] D. Ghosh, A. Thalapillil, and F. Ullah, *Phys. Rev. D* **103**, 023006 (2021), arXiv:2009.03363 [hep-ph].
- [27] J. Estes, M. Kavic, S. L. Liebling, M. Lippert, and J. H. Simonetti, *JCAP* **06**, 017 (2023), arXiv:2209.06060 [astro-ph.HE].
- [28] M. D. Diamond and D. E. Kaplan, *JHEP* **03**, 157 (2022), arXiv:2103.01850 [hep-ph].
- [29] R. Gervalle and M. S. Volkov, Supplemental Materials.
- [30] R. Gervalle and M. S. Volkov, in preparation.
- [31] Y. Nambu, *Nucl. Phys. B* **130**, 505 (1977).
- [32] R. Gervalle and M. S. Volkov, *Nucl. Phys. B* **984**, 115937 (2022), arXiv:2203.16590 [hep-th].
- [33] F. Hecht, *J. Numer. Math.* **20**, 251 (2012).
- [34] R. P. Geroch, *J. Math. Phys.* **11**, 2580 (1970).
- [35] R. Hansen, *J. Math. Phys.* **15**, 46 (1974).
- [36] G. Fodor, C. Hoenselaers, and Z. Perjes, *J. Math. Phys.* **30**, 2252 (1989).
- [37] G. Fodor, E. d. S. C. Filho, and B. Hartmann, *Phys. Rev. D* **104**, 064012 (2021), arXiv:2012.05548 [gr-qc].
- [38] N. Arkani-Hamed, L. Motl, A. Nicolis, and C. Vafa, *JHEP* **06**, 060 (2007), arXiv:hep-th/0601001.
- [39] Y. M. Cho and D. Maison, *Phys. Lett. B* **391**, 360 (1997), arXiv:hep-th/9601028.
- [40] R. Gervalle and M. S. Volkov, *Nucl. Phys. B* **987**, 116112 (2023), arXiv:2211.04875 [hep-th].
- [41] C. A. R. Herdeiro and E. Radu, *Phys. Rev. D* **107**, 064044 (2023), arXiv:2302.00016 [gr-qc].

SUPPLEMENTAL MATERIALS

S.1. DIMENSIONFUL AND DIMENSIONLESS QUANTITIES

We denote dimensionful quantities by boldfaced letters and the dimensionless ones by ordinary letters. The action of the bosonic part of the gravity-coupled electroweak theory is

$$\mathcal{S} = \frac{1}{c} \int \left(\frac{c^4}{16\pi\mathbf{G}} \mathbf{R} + \mathbf{L}_{\text{WS}} \right) \sqrt{-g} d^4x, \quad (1.1)$$

where the electroweak Lagrangian is usually chosen in the form

$$\begin{aligned} \mathbf{L}_{\text{WS}} = & -\frac{1}{4} \mathbf{W}_{\mu\nu}^a \mathbf{W}^{a\mu\nu} - \frac{1}{4} \mathbf{B}_{\mu\nu} \mathbf{B}^{\mu\nu} \\ & - (D_\mu \Phi)^\dagger D^\mu \Phi - \lambda (\Phi^\dagger \Phi - \Phi_0^2)^2. \end{aligned} \quad (1.2)$$

Here Φ_0 is the Higgs field vacuum expectation value and

$$\begin{aligned} \mathbf{W}_{\mu\nu}^a &= \partial_\mu \mathbf{W}_\nu^a - \partial_\nu \mathbf{W}_\mu^a + g\epsilon_{abc} \mathbf{W}_\mu^b \mathbf{W}_\nu^c, \\ \mathbf{B}_{\mu\nu} &= \partial_\mu \mathbf{B}_\nu - \partial_\nu \mathbf{B}_\mu, \\ D_\mu \Phi &= \left(\partial_\mu - \frac{ig'}{2} \mathbf{B}_\mu - \frac{ig}{2} \tau_a \mathbf{W}_\mu^a \right) \Phi, \end{aligned} \quad (1.3)$$

with $\partial_\mu = \partial/\partial x^\mu$. Denoting $g_0 = \sqrt{g^2 + g'^2}$ one can pass to dimensionless quantities by setting

$$\begin{aligned} g &= g_0 g, \quad g' = g_0 g', \quad \mathbf{W}_\mu^a = \frac{\Phi_0}{g} W_\mu^a, \\ \mathbf{B}_\mu &= \frac{\Phi_0}{g'} B_\mu, \quad \Phi = \Phi_0 \Phi, \quad \lambda = \frac{\beta}{8} g_0^2, \end{aligned} \quad (1.4)$$

while the spacetime coordinates $x^\mu = l_0 x^\mu$ with the length scale $l_0 = 1/(g_0 \Phi_0)$. The corresponding mass scale is $\mathbf{m}_0 = \hbar/(cl_0) = (\hbar/c) g_0 \Phi_0$.

The dimensionful electron charge is $e = \hbar c g_0 \times e$ with $e \equiv gg' = \sin\theta_w \cos\theta_w = 0.416$ and the fine structure constant

$$\begin{aligned} \alpha &= \frac{e^2}{4\pi\hbar c} = \frac{e^2}{4\pi} \hbar c g_0^2 \approx \frac{1}{137} \Rightarrow \\ \frac{1}{c g_0^2} &= \frac{e^2}{4\pi\alpha} \hbar = 1.89 \hbar, \quad \frac{1}{g_0} = \frac{\hbar c}{e} e = \frac{e}{4\pi\alpha} e. \end{aligned} \quad (1.5)$$

Injecting everything into (1.1) and introducing the dimensionless gravitational coupling,

$$\kappa = \frac{8\pi\mathbf{G}\Phi_0^2}{c^4}, \quad (1.6)$$

the action becomes $\mathcal{S} = \hbar \times \mathcal{S}$ with

$$\mathcal{S} = \frac{e^2}{4\pi\alpha} \int \left(\frac{1}{2\kappa} R + \mathcal{L}_{\text{WS}} \right) \sqrt{-g} d^4x, \quad (1.7)$$

and

$$\begin{aligned} \mathcal{L}_{\text{WS}} = & -\frac{1}{4g^2} W_{\mu\nu}^a W^{a\mu\nu} - \frac{1}{4g'^2} B_{\mu\nu} B^{\mu\nu} \\ & - (D_\mu \Phi)^\dagger D^\mu \Phi - \frac{\beta}{8} (\Phi^\dagger \Phi - 1)^2. \end{aligned} \quad (1.8)$$

This is the action in Eq.(1) in the main text.

The Z-boson mass is $m_z = 1/\sqrt{2}$ whose dimensionful version

$$\mathbf{m}_z = \frac{\mathbf{m}_0}{\sqrt{2}} = \frac{\hbar g_0 \Phi_0}{\sqrt{2}c} = 91.18 \text{ GeV}/c^2 \quad (1.9)$$

determines the mass scale $\mathbf{m}_0 = 128.9 \text{ GeV}/c^2$, and the length scale $l_0 = 1.53 \times 10^{-16} \text{ cm}$, hence

$$\kappa = \frac{4e^2}{\alpha} \left(\frac{\mathbf{m}_z}{\mathbf{M}_{\text{Pl}}} \right)^2 = 5.42 \times 10^{-33}. \quad (1.10)$$

The dimensionful version of the ADM mass is determined from the asymptotic form of the g_{00} metric coefficient,

$$-g_{00} = 1 - \frac{2M}{r} + \dots = 1 - \frac{2\mathbf{G}\mathbf{M}}{c^2 r} + \dots, \quad (1.11)$$

where $r = l_0 r$ hence

$$\begin{aligned} \frac{\mathbf{M}}{\mathbf{m}_0} &= \frac{c^2 l_0}{\mathbf{G} \mathbf{m}_0} M = \frac{8\pi}{\kappa} \times \frac{M}{\hbar c g_0^2} \\ &= \frac{e^2}{4\pi\alpha} \times \frac{8\pi}{\kappa} M \equiv \frac{e^2}{4\pi\alpha} \times \mathcal{M}. \end{aligned} \quad (1.12)$$

S.2. FIELD EQUATIONS

Varying the action (1.7) with respect to the EW fields gives the equations,

$$\begin{aligned} \nabla^\mu B_{\mu\nu} &= g'^2 \frac{i}{2} (\Phi^\dagger D_\nu \Phi - (D_\nu \Phi)^\dagger \Phi), \\ \mathcal{D}^\mu W_{\mu\nu}^a &= g^2 \frac{i}{2} (\Phi^\dagger \tau^a D_\nu \Phi - (D_\nu \Phi)^\dagger \tau^a \Phi), \\ D_\mu D^\mu \Phi - \frac{\beta}{4} (\Phi^\dagger \Phi - 1) \Phi &= 0, \end{aligned} \quad (2.1)$$

with $\mathcal{D}_\mu W_{\alpha\beta}^a = \nabla_\mu W_{\alpha\beta}^a + \epsilon_{abc} W_\mu^b W_{\alpha\beta}^c$ where ∇_μ is the geometrical covariant derivative with respect to the spacetime metric $g_{\mu\nu}$. Varying the action with respect to the latter yields the Einstein equations

$$G_{\mu\nu} = \kappa T_{\mu\nu}, \quad (2.2)$$

with the energy-momentum tensor

$$\begin{aligned} T_{\mu\nu} = & \frac{1}{g^2} W_{\mu\sigma}^a W_{\nu}^{a\sigma} + \frac{1}{g'^2} B_{\mu\sigma} B_{\nu}^{\sigma} \\ & + (D_\mu \Phi)^\dagger D_\nu \Phi + (D_\nu \Phi)^\dagger D_\mu \Phi + g_{\mu\nu} \mathcal{L}_{\text{WS}}. \end{aligned} \quad (2.3)$$

The vacuum is defined as the configuration with $T_{\mu\nu} = 0$. Modulo gauge transformations, it can be chosen as

$$W_\mu^a = B_\mu = 0, \quad \Phi = \begin{pmatrix} 0 \\ 1 \end{pmatrix}, \quad g_{\mu\nu} = \eta_{\mu\nu}, \quad (2.4)$$

where $\eta_{\mu\nu} = \text{diag}[-1, 1, 1, 1]$ is the Minkowski metric. Allowing for small fluctuations around the vacuum and linearizing the field equations with respect to the fluctuations, gives the perturbative mass spectrum containing the massless photon, massless graviton, and the massive Z, W and Higgs bosons with dimensionless masses

$$m_Z = \frac{1}{\sqrt{2}}, \quad m_W = g m_Z, \quad m_H = \sqrt{\beta} m_Z. \quad (2.5)$$

S.3. GAUGE TRANSFORMATIONS

The action (1.7) is invariant under $SU(2) \times U(1)$ gauge transformations

$$\Phi \rightarrow \mathcal{U} \Phi, \quad \mathcal{W} \rightarrow \mathcal{U} \mathcal{W} \mathcal{U}^{-1} + i \mathcal{U} \partial_\mu \mathcal{U}^{-1} dx^\mu, \quad (3.1)$$

with

$$\mathcal{W} = \frac{1}{2} (B_\mu + \tau^a W_\mu^a) dx^\mu, \quad \mathcal{U} = \exp \left(\frac{i}{2} \Sigma + \frac{i}{2} \tau^a \theta^a \right),$$

where Σ and θ^a are functions of x^μ .

The ansatz for the electroweak fields in Eq.(6) in the main text is

$$\begin{aligned} W &= T_2 (F_1 dr + F_2 d\vartheta) + \nu (T_3 F_3 - T_1 F_4) d\varphi, \\ B &= \nu Y d\varphi, \quad \Phi = \begin{pmatrix} \phi_1 \\ \phi_2 \end{pmatrix}, \end{aligned} \quad (3.2)$$

with $\nu = -n/2$. It keeps its form under gauge transformations generated by $\mathcal{U} = \exp \{i\chi(r, \vartheta) T_2\}$, whose effect is

$$\begin{aligned} F_1 &\rightarrow F_1 + \partial_r \chi, & F_2 &\rightarrow F_2 + \partial_\vartheta \chi, & Y &\rightarrow Y, \\ F_3 &\rightarrow F_3 \cos \chi - F_4 \sin \chi, \\ F_4 &\rightarrow F_4 \cos \chi + F_3 \sin \chi, \\ \phi_1 &\rightarrow \phi_1 \cos(\chi/2) + \phi_2 \sin(\chi/2), \\ \phi_2 &\rightarrow \phi_2 \cos(\chi/2) - \phi_1 \sin(\chi/2). \end{aligned} \quad (3.3)$$

The fields in (3.2) are singular at the symmetry axis. To remove the singularity, one sets

$$\begin{aligned} F_1 &= -\frac{H_1(r, \vartheta)}{r\sqrt{N}}, & F_2 &= H_2(r, \vartheta), \\ F_3 &= \cos \vartheta + H_3(r, \vartheta) \sin \vartheta, & F_4 &= H_4(r, \vartheta) \sin \vartheta, \\ Y &= \cos \vartheta + y(r, \vartheta) \sin \vartheta. \end{aligned} \quad (3.4)$$

The gauge transformation generated by

$$\mathcal{U}_\pm = e^{-i\nu\varphi T_3} e^{-i\vartheta T_2} e^{\pm i\nu\varphi/2} \quad (3.5)$$

brings the $SU(2)$ field to the form

$$\begin{aligned} W &= T_\varphi \left(-\frac{H_1}{r\sqrt{N}} dr + (H_2 - 1) d\vartheta \right) \\ &+ \nu (T_r H_3 + T_\vartheta (1 - H_4)) \sin \vartheta d\varphi, \end{aligned} \quad (3.6)$$

where $T_r = T_1 \sin \vartheta \cos(\nu\varphi) + T_2 \sin \vartheta \sin(\nu\varphi) + T_3 \cos \vartheta$ and $T_\vartheta = \partial_\vartheta T_r$, $T_\varphi = \partial_\varphi T_r / (\nu \sin \vartheta)$. This field is φ -dependent but regular at the symmetry axis, owing to the boundary conditions defined in Eq.(6.1) below (see [40] for details). The $U(1)$ and Higgs fields become

$$\begin{aligned} B_\pm &= \nu (\cos \vartheta \pm 1 + y \sin \vartheta) d\varphi, \\ \Phi_\pm &= e^{\pm i\nu\varphi/2} \begin{pmatrix} (\phi_1 \cos(\vartheta/2) - \phi_2 \sin(\vartheta/2)) e^{-i\nu\varphi/2} \\ (\phi_1 \sin(\vartheta/2) + \phi_2 \cos(\vartheta/2)) e^{+i\nu\varphi/2} \end{pmatrix}, \end{aligned} \quad (3.7)$$

where the upper “+” and lower “-” signs correspond to two local gauges used, respectively, in the southern and northern hemi-spheres. These two gauges are related to each other in the equatorial region by the $U(1)$ transformation with $\mathcal{U} = \exp(i\nu\varphi)$ (see [40] for details). When expressed in these two local gauges, the $U(1)$ and Higgs fields are everywhere regular.

The above formulas suggest that $\nu = -n/2$ should be integer. However, it can be half-integer as well. In that case the φ -dependent part of T_r changes sign under $\varphi \rightarrow \varphi + 2\pi$, but the correct sign can be restored by the global gauge transformation generated by $\mathcal{U} = \tau_3$ or $\mathcal{U} = -\tau_3$ whose effect is

$$T_1 \rightarrow -T_1, \quad T_2 \rightarrow -T_2, \quad (3.8)$$

so that the field (3.6) does not change. Similarly, if ν is half-integer then the lower component of Φ_+ and the upper component of Φ_- change sign under $\varphi \rightarrow \varphi + 2\pi$, but the correct sign can be restored by the global gauge transformation generated by $\mathcal{U} = \tau_3$ and $\mathcal{U} = -\tau_3$, respectively. The fields (3.7) then remain invariant. As a result, all integer values of n are allowed.

S.4. DIFFEOMORPHISMS

The line element in Eq.(6) of the main text

$$\begin{aligned} ds^2 &= -e^{2U} N(r) dt^2 + e^{-2U} dl^2, \\ dl^2 &= e^{2K} \left[\frac{dr^2}{N(r)} + r^2 d\vartheta^2 \right] + e^{2S} r^2 \sin^2 \vartheta d\varphi^2, \end{aligned} \quad (4.1)$$

keeps its form under diffeomorphisms $r \rightarrow \tilde{r} = \tilde{r}(r)$ whose effect is $U \rightarrow \tilde{U}$, $N \rightarrow \tilde{N}$, $K \rightarrow \tilde{K}$, $S \rightarrow \tilde{S}$, where

$$\begin{aligned} \frac{dr}{r\sqrt{N}} &= \frac{d\tilde{r}}{\tilde{r}\sqrt{\tilde{N}}}, & e^U \sqrt{N} &= e^{\tilde{U}} \sqrt{\tilde{N}}, \\ r\sqrt{N} e^K &= \tilde{r}\sqrt{\tilde{N}} e^{\tilde{K}}, & r\sqrt{N} e^S &= \tilde{r}\sqrt{\tilde{N}} e^{\tilde{S}}. \end{aligned} \quad (4.2)$$

This symmetry can be fixed by making a specific choice for the auxiliary function $N(r)$, for example one can set

$N(r) = 1$. We choose $N(r) = 1 - r_H/r$ for the non-extremal solutions, then $r = r_H$ corresponds to the position of the event horizon. However, since r is not the Schwarzschild coordinate, the parameter r_H does not have a direct physical meaning, although its value determine the horizon area. One has $r_H \in [0, r_H^0]$ and when $r_H \rightarrow 0$, the solutions approach the extremal limit with a non-zero horizon area, while for $r_H \rightarrow r_H^0$ they merge with the RN solution and one has $r_H^0 = r_+ - r_-$ where $r_{\pm} = M \pm \sqrt{M^2 - Q^2}$ are the two RN horizons.

For the extremal solutions we make the choice $N(r) = k(r) \times (1 - r_H/r)^2$ with

$$k(r) = 1 - \frac{\Lambda}{3} \left[r^2 + 2r_H r + 3r_H^2 \right] \times \frac{1 + r_H^4}{1 + r^4}. \quad (4.3)$$

The horizon is again at $r = r_H$ and it is degenerate so that the surface gravity vanishes. The parameter r_H again does not have a direct physical meaning and is not related anymore to the horizon area, so that, for example, one can set $r_H = 1$. However, for the extremal solutions in phase I which have a spherical horizon it is convenient to choose $r_H = r_{\text{ex}}$ where r_{ex} is the radius of the extremal RNdS solution described by Eq.(3) in the main text. In this case the radial coordinate r coincides at the horizon with the Schwarzschild coordinate r and the function $N(r)$ has the same limit as $N(r)$ for the extremal RNdS solution. For extremal solutions in phase II one can set $r_H = \text{const}$.

S.5. CHARGE AND CURRENTS

The electromagnetic and Z fields are defined according to Nambu [31],

$$\begin{aligned} \mathcal{F}_{\mu\nu} &= \frac{g}{g'} B_{\mu\nu} - \frac{g'}{g} n^a W_{\mu\nu}^a, \\ \mathcal{Z}_{\mu\nu} &= B_{\mu\nu} + n^a W_{\mu\nu}^a, \end{aligned} \quad (5.1)$$

where $n^a = \Phi^\dagger \tau^a \Phi / (\Phi^\dagger \Phi)$. The 2-form

$$\mathcal{F} = \frac{1}{2} \mathcal{F}_{\mu\nu} dx^\mu \wedge dx^\nu, \quad (5.2)$$

is closed in the Higgs vacuum where $\mathcal{F}_{\mu\nu}$ reduces to the usual electromagnetic field tensor. Away from the Higgs vacuum the form \mathcal{F} is not necessarily closed since in this case there is no reason for Maxwell equations to apply. Defining the dual field tensor,

$$\tilde{\mathcal{F}}^{\mu\nu} = \frac{1}{2\sqrt{-g}} \epsilon^{\mu\nu\alpha\beta} \mathcal{F}_{\alpha\beta}, \quad (5.3)$$

The conserved electric current and magnetic densities can be defined as

$$\mathcal{J}^\mu = \frac{1}{4\pi} \frac{1}{\sqrt{-g}} \partial_\nu (\sqrt{-g} \mathcal{F}^{\mu\nu}). \quad (5.4)$$

$$\tilde{\mathcal{J}}^\mu = \frac{1}{4\pi} \frac{1}{\sqrt{-g}} \partial_\nu (\sqrt{-g} \tilde{\mathcal{F}}^{\mu\nu}). \quad (5.5)$$

The flux of \mathcal{F} through a two-sphere S^2 at spatial infinity defines the conserved magnetic charge,

$$P = \frac{1}{4\pi} \oint_{S^2} \mathcal{F}. \quad (5.6)$$

Since $\mathcal{F}_{\mu\nu}$ consists of two parts determined by the contribution of $B_{\mu\nu}$ and of $W_{\mu\nu}^a$, the magnetic charge splits,

$$P = P_{U(1)} + P_{SU(2)}, \quad (5.7)$$

with

$$\begin{aligned} P_{U(1)} &= \frac{1}{4\pi} \frac{g}{g'} \oint_{S^2} \frac{1}{2} B_{\mu\nu} dx^\mu \wedge dx^\nu \\ &= \frac{g}{g'} \frac{1}{4\pi} \oint_{S^2} dB = \frac{g}{g'} \frac{n}{2} = g^2 \frac{n}{2e} = g^2 P, \end{aligned} \quad (5.8)$$

where we used the expression for the B -field in (3.2),(3.4) and the boundary conditions specified below in (6.1). The integral here does not depend on the radius of the sphere hence this part of the charge is always contained inside the black hole.

The remaining part of the charge,

$$P_{SU(2)} = P - P_{U(1)} = g'^2 P, \quad (5.9)$$

is not always contained inside the black hole. Its part distributed outside can be obtained by subtracting the flux at the horizon from flux at infinity,

$$\begin{aligned} 4\pi P_h &= \oint_{r \rightarrow \infty} \mathcal{F} - \oint_{r=r_H} \mathcal{F} = \int_{r>r_H} d\mathcal{F} \\ &= \int_{r>r_H} \frac{1}{2} \epsilon^{ijk} \partial_i \mathcal{F}_{jk} d^3x = \int_{r>r_H} \tilde{J}^0 \sqrt{-g} d^3x. \end{aligned} \quad (5.10)$$

Since the form $\mathcal{F}_{\mu\nu}$ is not necessarily closed, the latter integral can be non-zero. One has

$$\mathcal{F}_{\mu\nu} = F_{\mu\nu} + e\psi_{\mu\nu}, \quad (5.11)$$

where $F_{\mu\nu} = \partial_\mu A_\nu - \partial_\nu A_\mu$ is a closed form while the rest (the t'Hooft tensor) is not closed,

$$\psi_{\mu\nu} = -\epsilon_{abc} n^a \mathcal{D}_\mu n^b \mathcal{D}_\nu n^c, \quad (5.12)$$

with $\mathcal{D}_\mu n^a = \partial_\mu n^a + \epsilon_{abc} W_\mu^b n^c$. This tensor is made of massive fields and approaches zero exponentially fast at infinity, therefore,

$$\begin{aligned} 4\pi P_h &= e \int_{r>r_H} \frac{1}{2} \epsilon^{ijk} \partial_i \psi_{jk} d^3x \\ &= -e \oint_{S^2, r=r_H} \frac{1}{2} \psi_{ik} dx^i \wedge dx^k. \end{aligned} \quad (5.13)$$

The tensor $F_{\mu\nu}$ defines another conserved current density,

$$J^\mu = \frac{1}{4\pi} \frac{1}{\sqrt{-g}} \partial_\nu (\sqrt{-g} F^{\mu\nu}). \quad (5.14)$$

This is a neutral current which sources the F,Z fields and is responsible for the formation of vortices at the horizon (the corona). Integrating the current densities \mathcal{J}^μ and J^μ over a 2-surface gives currents.

In the static case, denoting $\mathcal{N} = \sqrt{-g_{00}}$, the relation (5.4) (similarly for (5.14)) can be represented in the form language as

$$d(\mathcal{N} * \mathcal{F}) = 4\pi \mathcal{N} * \mathcal{J} \quad (5.15)$$

where $*$ denotes the Hodge duality operator on the space-like 3-surface. Both sides of this relation are 2-forms. Integrating over a 2-surface Σ and applying Green's theorem yields

$$\frac{1}{4\pi} \int_{\partial\Sigma} \mathcal{N} * \mathcal{F} = \int_{\Sigma} \mathcal{N} * \mathcal{J} \equiv \mathcal{I}. \quad (5.16)$$

Here on the left is the circulation of the magnetic field along the boundary $\partial\Sigma$, hence on the right is the total current through Σ .

In the situation considered in the main text the currents are along the azimuthal direction, hence they flow through planes of constant φ . The above definition then implies that the total azimuthal current in the upper half-space, $\vartheta < \pi/2$, is

$$\mathcal{I}_+ = \int_{r_{\text{H}}}^{\infty} dr \int_0^{\pi/2} d\vartheta \sqrt{-g} \mathcal{J}^\varphi; \quad (5.17)$$

similarly for the current I associated with of J^φ . A similar integral with $\vartheta \in [\pi/2, \pi]$ yields the current \mathcal{I}_- in the lower half-space. Since \mathcal{J}^φ is antisymmetric with respect to the equatorial plane, the total current is zero, $\mathcal{I}_+ + \mathcal{I}_- = 0$. The dimensionful current expressed in amperes is

$$\mathbf{I} = c\Phi_0 \mathcal{I} = \frac{e}{4\pi\alpha} \frac{e}{t_0} \mathcal{I} = 1.42 \times 10^8 \times \mathcal{I} \text{ A}, \quad (5.18)$$

where $t_0 = l_0/c = 5.1 \times 10^{-27}$ sec.

S.6. BOUNDARY CONDITIONS AND NUMERICAL PROCEDURE

The axially symmetric EWS fields are the line element in (4.1) and the electroweak fields in (3.2),(3.4) expressed in terms of 10 functions $U, K, S, H_1, H_2, H_3, H_4, y, \phi_1, \phi_2$ depending on r, ϑ . The fields in (3.2),(3.4) have a residual U(1) gauge invariance (3.3) that we fix by imposing the gauge condition $r\sqrt{N}\partial_r H_1 = \partial_\vartheta H_2$. This gives 10 elliptic equations whose solutions fulfil also the first order gravitational constraints owing to the boundary conditions described by Eq.(6.1) below.

We use the compact radial variable $x \in [0, 1]$ such that $r = \sqrt{r_{\text{H}}^2 + x^2/(1-x)^2}$ and assume the reflection invariance of the energy density under $\vartheta \rightarrow \pi - \vartheta$ to restrict the

range to $\vartheta \in [0, \pi/2]$. The following boundary conditions at the borders of the integration domain are imposed:

$$\begin{aligned} \underline{\text{axis, } \vartheta = 0} : & \quad \partial_\vartheta = 0 \text{ for } U, S, H_2, H_4, \phi_2; \\ & \quad K - S = H_1 = H_3 = y = \phi_1 = 0; \\ \underline{\text{equator, } \vartheta = \pi/2} : & \quad \partial_\vartheta = 0 \text{ for } U, K, S, H_2, H_4, \phi_2; \\ & \quad H_1 = H_3 = y = \phi_1 = 0; \\ \underline{\text{horizon, } x = 0} : & \quad H_1 = 0 : \partial_x = 0 \text{ for the rest} \\ \underline{\text{infinity, } x = 1} : & \quad \phi_2 = 1; 0 \text{ for the rest.} \end{aligned} \quad (6.1)$$

It turns out that these boundary conditions automatically imply that at the symmetry axis one has $H_2 = H_4$ and $\partial_\vartheta K = 0$, as needed for the regularity.

We solve the field equations with these boundary conditions to determine the components of the ‘‘state vector’’

$$\Psi = [H_1, H_2, H_3, H_4, y, \phi_1, \phi_2, U, K, S], \quad (6.2)$$

which are functions of r, ϑ . We solve the equations with the FreeFem numerical solver based on the finite element method [33]. This solver uses the weak form of differential equations obtained by transforming them into integral equations, expanding with respect to basis functions obtained by triangulating the integration domain, and handling the non-linearities with the Newton-Raphson procedure. The quality of the solutions is checked by monitoring the virial relation that should hold on-shell,

$$v \equiv \int_{r>r_{\text{H}}} T^\mu_\nu \nabla_\mu \zeta^\nu \sqrt{-g} d^3x = 0, \quad (6.3)$$

where $\zeta_\mu dx^\mu = r e^{K-U} dr$ and T^μ_ν is the EW energy-momentum tensor (2.3). For a domain triangulation by 100×60 elements we typically obtain $v \sim 10^{-7}$.

S.7. HORIZON MASS

The horizon radius of the RN solution with the magnetic charge P and mass M is $r_h = M + \sqrt{M^2 - Q^2}$ where $Q^2 = (\kappa/2)P^2$, hence

$$M = \frac{r_h}{2} + \frac{Q^2}{2r_h} = \frac{r_h}{2} + \frac{\kappa P^2}{4r_h}. \quad (7.1)$$

On the other hand, the total magnetic charge consists of the U(1) part and SU(2) part, $P = P_{\text{U}(1)} + P_{\text{SU}(2)}$ with $P_{\text{U}(1)} = g^2 P$ and $P_{\text{SU}(2)} = g'^2 P$ and one has

$$P^2 = \frac{1}{g^2} P_{\text{U}(1)}^2 + \frac{1}{g'^2} P_{\text{SU}(2)}^2. \quad (7.2)$$

This formula is important: although P is the sum of two charges, P^2 is not the square of the sum because the two charges are of different nature and only the square of each charge contributes to the energy.

The magnetic charge of a hairy black hole splits as $P = P_{\text{H}} + P_{\text{h}}$ where P_{H} is the charge contained inside

the black hole and P_h is the charge contained outside in the hair defined by (5.10). The hair charge is always a part of the non-Abelian charge $P_{\text{SU}(2)}$, hence

$$P_h = \tilde{\lambda} P_{\text{SU}(2)}, \quad P_H = P_{\text{U}(1)} + (1 - \tilde{\lambda}) P_{\text{SU}(2)}, \quad (7.3)$$

where the parameter $\tilde{\lambda}$ varies from zero for black holes which bifurcate with RN till unity for the extremal black holes in phase I. Comparing with (7.2), the square of the charge contained inside the black hole is computed according the rule

$$\begin{aligned} P_H^2 &= \frac{1}{g^2} P_{\text{U}(1)}^2 + \frac{(1 - \tilde{\lambda})^2}{g'^2} P_{\text{SU}(2)}^2 \\ &= (g^2 + (1 - \tilde{\lambda})^2 g'^2) P^2. \end{aligned} \quad (7.4)$$

Therefore, *defining* the size of a hairy black hole with a horizon area A_H as $r_h = \sqrt{A_H/(4\pi)}$ and comparing with (7.1), the horizon mass is

$$M_H = \frac{r_h}{2} + \frac{\kappa P_H^2}{4r_h} = \frac{r_h}{2} + \frac{\kappa P^2}{4r_h} (g^2 + (1 - \tilde{\lambda})^2 g'^2). \quad (7.5)$$

For the hairy solutions bifurcating with the RN branch one has $\tilde{\lambda} = 0$ and the formula reduces to (7.1). For the extremal hairy solutions in phase I one has $\tilde{\lambda} = 1$ and

$$M_H = \frac{r_h}{2} + \frac{\kappa g^2 P^2}{4r_h} = \frac{r_h}{2} + g^2 \frac{Q^2}{2r_h}. \quad (7.6)$$

Notice finally that $P_h = \tilde{\lambda} P_{\text{SU}(2)} = \tilde{\lambda} g'^2 P \equiv \lambda P$ hence $\tilde{\lambda} = \lambda/g'^2$ where $\lambda = P_h/P$ is used in the main text.

S.8. QUADRUPOLE MOMENTS

Far away from the horizon all massive fields approach vacuum values and one has

$$B_\mu = W_\mu^3 \equiv e A_\mu, \quad W_\mu^1 = W_\mu^2 = 0, \quad \Phi = \begin{pmatrix} 0 \\ 1 \end{pmatrix}, \quad (8.1)$$

hence the Einstein-Weinberg-Salam theory reduces to the electrovacuum,

$$\mathcal{L} = \frac{1}{2\kappa} R - \frac{1}{4} F_{\mu\nu} F^{\mu\nu}, \quad (8.2)$$

where $F_{\mu\nu} = \partial_\mu A_\nu - \partial_\nu A_\mu$. The solutions approach at large distances the magnetic RN configuration of mass M and charge $Q = \sqrt{\kappa/2} P$. Choosing the gauge where $N(r) = 1$, the line element in (4.1) becomes

$$\begin{aligned} ds^2 &= -e^{2U} dt^2 + e^{-2U} dl^2, \\ dl^2 &\equiv h_{ik} dx^i dx^k = e^{2K} (dr^2 + r^2 d\vartheta^2) + r^2 e^{2S} \sin^2 \vartheta d\varphi^2, \end{aligned} \quad (8.3)$$

while the purely magnetic Maxwell field $F_{\mu\nu}$ can be expressed in terms of a magnetic potential Ψ as

$$\sqrt{\frac{\kappa}{2}} F_{ik} = e^{-2U} \sqrt{h} \epsilon_{iks} \partial^s \Psi. \quad (8.4)$$

Our solutions in the far field region reduce to

$$\begin{aligned} e^{2U} &= e^{2\delta U} \frac{x^2 - \mu^2}{(x + M)^2}, & e^K &= e^{\delta K} \left(1 - \frac{\mu^2}{4r^2} \right), \\ e^S &= e^{\delta S} \left(1 - \frac{\mu^2}{4r^2} \right), & \Psi &= \frac{Q}{x + M} + \delta\Psi, \end{aligned} \quad (8.5)$$

with $x = r + \mu^2/(4r)$ and $\mu^2 = M^2 - Q^2$. In the leading order this is the RN solution in the isotropic coordinates, while the subleading terms describe deviations from the RN background,

$$\begin{aligned} \delta S &= -\frac{s_2}{2r^2} + \dots, \\ \delta K &= s_2 \frac{2 \sin^2 \vartheta - 1}{2r^2} + \dots, \\ \delta U &= \frac{Q_g (1 - 3 \cos^2 \vartheta) - M s_2/3}{2r^3} + \dots, \\ \delta \Psi &= \frac{Q_m (1 - 3 \cos^2 \vartheta) + Q s_2/3}{2r^3} + \dots, \end{aligned} \quad (8.6)$$

where Q_g, Q_m, s_2 are integration constants and the dots denote higher order terms. The values of these constants can be determined from our numerical solutions, taking into account that the latter are obtained in a different radial gauge where $N(r) \neq 1$.

Introducing the Ernst potential,

$$\mathcal{E} = e^{2U} - \Psi^2, \quad (8.7)$$

the gravitational Q_G and magnetic Q_M quadrupole moments defined within the Geroch-Hansen approach [34, 35] are determined by the behaviour of

$$\xi = \frac{1 - \mathcal{E}}{1 + \mathcal{E}}, \quad q = \frac{2\Psi}{1 + \mathcal{E}} \quad (8.8)$$

near spatial infinity. This requires [36, 37] passing to the Weyl coordinates where

$$dl^2 = e^{2K(\rho, z)} (d\rho^2 + dz^2) + \rho^2 d\varphi^2, \quad (8.9)$$

(the function K can be expressed in terms of K, S) and considering the asymptotic expansions at the symmetry axis, $\rho = 0$, for $z \rightarrow \infty$,

$$\xi = \sum_{k \geq 0} \frac{a_k}{z^{k+1}}, \quad q = \sum_{k \geq 0} \frac{b_k}{z^{k+1}}, \quad (8.10)$$

from where $Q_G = -a_2$, $Q_M = -b_2$. Transforming the 3-metric in (8.3) to the Weyl coordinates, computing the potentials ξ and q and expanding them according to (8.10) yields

$$Q_G = -Q_g - \frac{2}{3} M s_2, \quad Q_M = Q_m - \frac{2}{3} Q s_2. \quad (8.11)$$

S.9. BEYOND AXIAL SYMMETRY

Although this is not the main subject of this work, we consider also non-axially symmetric solutions by adapting the perturbative approach of [18]. The idea is to expand around the RN solution up to the second order terms and then minimize the energy.

Passing to the unitary gauge where the Higgs field $\Phi^{\text{tr}} = (0, \phi)$ with real-valued ϕ , defining the complex-valued vector field $w_\mu = (W_\mu^1 + iW_\mu^2)/g$ with the strength $w_{\mu\nu} = D_\mu w_\nu - D_\nu w_\mu$ where $D_\mu = \nabla_\mu + iW_\mu^3$, the EW Lagrangian (1.8) assumes the form

$$-\mathcal{L}_{\text{EW}} = \frac{1}{4g'^2}(B_{\mu\nu})^2 + \frac{1}{4g^2}(W_{\mu\nu}^3)^2 + \frac{1}{4}|w_{\mu\nu}|^2 \quad (9.1)$$

$$+ (\partial_\mu \phi)^2 + \frac{1}{4}(g^2|w_\mu|^2 + (B_\mu - W_\mu^3)^2)\phi^2 + \frac{\beta}{8}(\phi^2 - 1)^2.$$

Here $B_{\mu\nu} = \partial_\mu B_\nu - \partial_\nu B_\mu$ and

$$W_{\mu\nu}^3 = \partial_\mu W_\nu^3 - \partial_\nu W_\mu^3 + g^2\psi_{\mu\nu},$$

$$\psi_{\mu\nu} = \frac{i}{2}(w_\mu \bar{w}_\nu - w_\nu \bar{w}_\mu). \quad (9.2)$$

The electromagnetic and Z-fields (5.1) then become

$$e\mathcal{F}_{\mu\nu} = g^2 B_{\mu\nu} + g'^2 W_{\mu\nu}^3 \equiv eF_{\mu\nu} + e^2\psi_{\mu\nu},$$

$$\mathcal{Z}_{\mu\nu} = B_{\mu\nu} - W_{\mu\nu}^3 \equiv Z_{\mu\nu} - g^2\psi_{\mu\nu}, \quad (9.3)$$

where $F_{\mu\nu} = \partial_\mu A_\nu - \partial_\nu A_\mu$ and $Z_{\mu\nu} = \partial_\mu Z_\nu - \partial_\nu Z_\mu$ with

$$eA_\mu = g^2 B_\mu + g'^2 W_\mu^3, \quad Z_\mu = B_\mu - W_\mu^3. \quad (9.4)$$

The WS equations (2.1) assume the form

$$\nabla^\mu F_{\nu\mu} = 4\pi J_\nu, \quad \nabla^\mu Z_{\nu\mu} + \frac{\phi^2}{2} Z_\nu = -4\pi \frac{g}{g'} J_\nu,$$

$$D^\mu w_{\mu\nu} + i(g^2\psi_{\nu\sigma} + gg'F_{\nu\sigma} - g^2Z_{\nu\sigma})w^\sigma = \frac{g^2\phi^2}{2}w_\nu,$$

$$\nabla^\mu \nabla_\mu \phi = \frac{1}{4}(g^2 w_\mu \bar{w}^\mu + Z_\mu Z^\mu)\phi + \frac{\beta}{4}(\phi^2 - 1)\phi. \quad (9.5)$$

Here the gauge covariant derivative can be written in the form $D_\mu = \nabla_\mu + i(eA_\mu - g^2Z_\mu)$ and the current is

$$4\pi J_\nu = e\nabla^\sigma \psi_{\sigma\nu} + e\Im(\bar{w}^\sigma w_{\sigma\nu}). \quad (9.6)$$

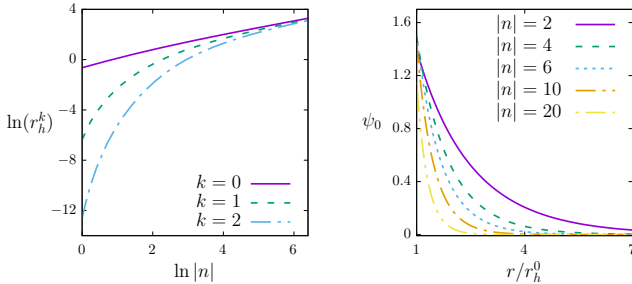


Figure 6. The RN horizon size $r_h^k(n)$ for which there exists a k -node zero mode $\psi_k(r)$ (left) and the profile of the fundamental zero mode $\psi_0(r)$ (right).

It should be emphasized that $F_{\mu\nu}$ has the potential, A_μ , while $\mathcal{F}_{\mu\nu}$ given by (5.1) and used in the main text to define \mathcal{J}_ν , $\tilde{\mathcal{J}}_\nu$ is not always closed,

$$\mathcal{F}_{\mu\nu} = \partial_\mu A_\nu - \partial_\nu A_\mu + e\psi_{\mu\nu}. \quad (9.7)$$

This is exactly the same relation as in (5.11) because the tensor $\psi_{\mu\nu}$ defined in (5.12) reduces in the unitary gauge precisely to $\psi_{\mu\nu}$ defined in (9.2).

Taking the divergence of (9.7) and comparing with (9.6) yields

$$4\pi\mathcal{J}_\nu = \nabla^\mu \mathcal{F}_{\nu\mu} = \nabla^\mu F_{\nu\mu} + e\nabla^\mu \psi_{\nu\mu}$$

$$= 4\pi J_\nu - e\nabla^\mu \psi_{\mu\nu} = e\Im(\bar{w}^\sigma w_{\sigma\nu}). \quad (9.8)$$

hence

$$J_\nu = \mathcal{J}_\nu + \frac{e}{4\pi} \nabla^\sigma \psi_{\sigma\nu}. \quad (9.9)$$

Eqs.(9.5) admit the solution

$$A_\mu dx^\mu = -\frac{n}{2e} \cos\vartheta d\varphi, \quad Z_\mu = w_\mu = 0, \quad \phi = 1, \quad (9.10)$$

assuming the background geometry to be RN. Expanding Eqs.(9.5) around this solution yields in the first order of perturbation theory

$$D^\mu w_{\mu\nu} + ieF_{\nu\sigma}w^\sigma = \frac{g^2}{2}w_\nu, \quad (9.11)$$

with $D_\mu = \nabla_\mu + ieA_\mu$ where A_μ is the same as in (9.10) (the fields Z_μ, ϕ also do not change in the first order). This equation admits a solution of the form

$$w_\mu dx^\mu = e^{i\omega t} \sum_{m \in [-j, j]} c_m w_m(r, \vartheta, \varphi), \quad (9.12)$$

$$w_m = \psi(r) (\sin\vartheta)^j \left(\tan\frac{\vartheta}{2}\right)^m e^{-im\varphi} (d\vartheta - i\sin\vartheta d\varphi),$$

if $n > 1$, while for $n < -1$ one has to replace $w_m \rightarrow \bar{w}_m$. The value $|n| = 1$ is excluded since w_m is then unbounded at the symmetry axis. One has $j = |n|/2 - 1$. The coefficients c_m are arbitrary and can be chosen to be real. The function $\psi(r)$ fulfills the equation

$$\left(-\frac{d^2}{dr_*^2} + N(r) \left[m_w^2 - \frac{|n|}{2r^2}\right]\right) \psi(r) = \omega^2 \psi(r), \quad (9.13)$$

with $dr_* = dr/N(r)$ where $N(r) = 1 - 2M/r + Q^2/r^2$ and $Q^2 = (\kappa n^2)/(8e^2)$. This equation admits normalizable solutions with $\omega^2 < 0$ (negative modes) if the horizon radius $r_h = M + \sqrt{M^2 - Q^2}$ is small. Therefore, small RN black holes are unstable with respect to the formation of the charged W-condensate, whereas large black holes are stable.

Varying r_h , one can detect critical values $r_h^k(n)$ for which instabilities just settle in as zero modes, that is normalizable solutions with $\omega = 0$. These solutions, $\psi_k(r)$,

are characterized by $k = 0, 1, 2, \dots$ nodes and they exist only for discrete values of the event horizon radius $r_h = r_h^k(n)$ shown in Fig.6. The functions $\psi_k(r)$ are finite at the horizon and decay exponentially fast at large r ; see Fig.6. Since $\omega = 0$, the solution (9.12) with $\psi(r) = \psi_k(r)$ describes static deformations of the RN black hole, the value $k = 0$ corresponding to the fundamental mode and $k > 0$ being the radial excitations.

Setting in (9.12) $\omega = 0$, the solution can be transformed to the form expressed by Eq.(4) of the main text, while (9.13) reduces to Eq.(5) of the main text. This solution is defined up to an overall sign which can be flipped by the gauge transformation generated by $\mathcal{U} = -\tau_3$, whose effect is $T_1 \rightarrow -T_1$ and $T_2 \rightarrow -T_2$, hence $w_\mu \rightarrow -w_\mu$ while the RN background does not change. It follows that there are two options: either w_μ does not change under $\varphi \rightarrow \varphi + 2\pi$ or it flips sign. Therefore, since $w_m \sim \exp(-im\varphi)$, the azimuthal number m can assume either only integer or only half-integer values. For example, if $j = 1$ then the two options are either $m = \pm 1/2$ or $m = 0, \pm 1$.

There is always an option containing the value $m = 0$ and it is possible to choose $c_m = \delta_{m0}$ since coefficients c_m are arbitrary within the linear perturbation theory. However, they are no longer arbitrary when the higher order corrections are taken into account, although the possibility to choose $c_m = \text{const.} \times \delta_{m0}$ always exists.

One has $\mathfrak{S}(\bar{w}^\sigma w_{\sigma\nu}) = 0$ for the solution (9.12) hence $4\pi J_\mu = e\nabla^\sigma \psi_{\sigma\mu}$ is tangential to the sphere, with non-zero components

$$J_\vartheta = \frac{e}{8\pi \sin \vartheta} \partial_\varphi |w_\mu|^2, \quad J_\varphi = -\frac{e \sin \vartheta}{8\pi} \partial_\vartheta |w_\mu|^2, \quad (9.14)$$

where

$$|w_\mu|^2 \equiv w_\mu \bar{w}^\mu = \frac{2}{r^2} |\psi(r)|^2 \times \Theta(\vartheta, \varphi), \quad (9.15)$$

$$\Theta(\vartheta, \varphi) = (\sin \vartheta)^{2j} \sum_{k,m} c_k c_m \left(\tan \frac{\vartheta}{2} \right)^{k+m} e^{i(k-m)\varphi}.$$

It follows from (9.14) that J^μ is orthogonal to the gradient of $|w_\mu|^2$, which is in turn orthogonal to the level lines of $|w_\mu|^2$. Therefore, the latter are parallel to J^μ .

The current is quadratic in w_μ , c_m and sources second order correction for the electromagnetic field, $f_{\mu\nu}$, second order Z_μ and second order $\delta\phi = \phi - 1$. Expanding (9.5) up to second order terms yields

$$\nabla^\mu f_{\nu\mu} = e \nabla^\sigma \psi_{\sigma\nu}, \quad (9.16a)$$

$$\nabla^\mu Z_{\nu\mu} + \frac{1}{2} Z_\nu = -g^2 \nabla^\sigma \psi_{\sigma\nu}, \quad (9.16b)$$

$$\nabla^\mu \nabla_\mu \delta\phi - \frac{\beta}{2} \delta\phi = \frac{g^2}{4} |w_\mu|^2. \quad (9.16c)$$

Solving these equations and injecting to (9.1), yields the

result containing terms up to fourth order,

$$\begin{aligned} -\mathcal{L}_{\text{EW}} &= \frac{1}{4} (gF_{\mu\nu} + g'Z_{\mu\nu})^2 + \frac{1}{4} (g'F_{\mu\nu} - gZ_{\mu\nu} + g\psi_{\mu\nu})^2 \\ &+ \frac{1}{4} |w_{\mu\nu}|^2 + \frac{g^2}{4} |w_\mu|^2 (1 + 2\delta\phi) + \frac{1}{4} (Z_\mu)^2 \\ &+ (\partial_\mu \delta\phi)^2 + \frac{\beta}{2} \delta\phi^2. \end{aligned} \quad (9.17)$$

Here $F_{\mu\nu} = \overset{0}{F}_{\mu\nu} + f_{\mu\nu}$ with $\overset{0}{F}_{\mu\nu}$ being the zeroth-order field corresponding to (9.10). Since the fields are static and purely magnetic, the energy density is $\mathcal{E} = -\mathcal{L}_{\text{EW}}$.

The procedure now is to solve Eqs.(9.16), compute the energy $E = \int \mathcal{E} \sqrt{-g} d^3x$, and then minimize it with respect to the coefficients c_m by keeping fixed the norm $\int w_\mu \bar{w}^\mu \sqrt{-g} d^3x$. Eqs.(9.16) can be solved with Green's functions, as was done in [18] where a simplified theory without Z , Φ was considered. However, we postpone this for future work since our main goal at present is to study axially-symmetric solutions. To get some idea of more general solutions, we use an approximate procedure, which nevertheless seems to capture the essential points. The key observation is that the energy density always contains the fourth order term $(\psi_{\mu\nu})^2 \sim |w_\mu|^4$. Therefore, we minimize

$$\langle |w_\mu|^4 \rangle \equiv \int |w_\mu|^4 \sqrt{-g} d^3x, \quad (9.18)$$

under the condition that the norm should be fixed,

$$\langle |w_\mu|^2 \rangle \equiv \int |w_\mu|^2 \sqrt{-g} d^3x = \text{const.} \quad (9.19)$$

One can also argue as follows. Eq. (9.16a) is fulfilled by

$$f_{\mu\nu} = -e\psi_{\mu\nu}. \quad (9.20)$$

This solution is not totally satisfactory since the form $\psi_{\mu\nu}$ is not closed, but we ignore this. Then the non-zero components are

$$f_{\vartheta\varphi} = -f_{\varphi\vartheta} = e \frac{n}{|n|} |\psi(r)|^2 \Theta(\vartheta, \varphi) \sin \vartheta, \quad (9.21)$$

which corresponds to a radial magnetic field of the same direction as the background field. This confirms the EW anti-Lenz law: the magnetic field induced by the condensate enhances the external field and is maximal where the condensate is maximal [20–23].

Injecting (9.20) to (9.17), integrating by parts, using Eqs.(9.16), and omitting the zeroth order order term yields

$$\begin{aligned} \mathcal{E} &= \frac{g^4}{4} (\psi_{\mu\nu})^2 + \frac{1}{4} |w_{\mu\nu}|^2 + \frac{g^2}{4} |w_\mu|^2 \\ &- \frac{g^2}{4} \psi^{\mu\nu} Z_{\mu\nu} + \frac{g^2}{4} |w_\mu|^2 \delta\phi, \end{aligned} \quad (9.22)$$

where

$$(\psi_{\mu\nu})^2 = \frac{1}{2} |w_\mu|^4, \quad |w_{\mu\nu}|^2 = 2N(r) \left| \frac{\psi'(r)}{\psi(r)} \right|^2 |w_\mu|^2. \quad (9.23)$$

We do not know what $Z_{\mu\nu}$ and $\delta\phi$ are, but if we simply ignore them and set to zero the second line in (9.22), then the integration gives

$$E = \text{const.} \times \langle |w_\mu|^4 \rangle + \text{const.} \times \langle |w_\mu|^2 \rangle. \quad (9.24)$$

The same result is obtained if we ignore only $Z_{\mu\nu}$ but use the approximate solution for $\delta\phi$ obtained by neglecting the derivatives in (9.16c), $\delta\phi = -g^2/(2\beta) |w_\mu|^2$. Of course, the energy obtained by genuinely solving the equations (9.16) should have a more complicated structure. The justification for the heuristic prescription (9.24) is that it is simple and gives what is expected – the “platonic” distribution of vortices on the horizon. Therefore, it seems that the prescription (9.24) gives correct results, even though it relies on approximations.

Using (9.15), the second term in (9.24) reduces to $\text{const.} \times E_2$ with

$$E_2 = \sum_{m \in [-j, j]} A_{j,m} c_m^2, \quad (9.25)$$

where

$$\begin{aligned} A_{j,m} &= \int_0^\pi (\sin \vartheta)^{2j+1} \left(\tan \frac{\vartheta}{2} \right)^{2m} d\vartheta \\ &= 2^{2j+1} \frac{\Gamma(j+1+m)\Gamma(j+1-m)}{\Gamma(2j+2)}. \end{aligned} \quad (9.26)$$

Similarly, after some algebra, the first term in (9.24) reduces to $\text{const.} \times E_4$ with

$$E_4 = \sum_{k,m,l} A_{2j,k+1} c_m c_k c_l c_{k+1-m}. \quad (9.27)$$

It is assumed here that $c_m = 0$ if $|m| > j$. Therefore, omitting constant factors, the problem reduces to minimization with respect to c_m of

$$E = E_4 + \mu (E_2 - 1), \quad (9.28)$$

where μ is the Lagrange multiplier.

Assuming for example that $n = 10$ hence $j = 4$ and $m = -4, -3, \dots, 4$, so that there are 9 coefficients c_m to find. Their values corresponding to the absolute minimum of E determine the function $|w_\mu|^2$ in (9.15), whose value at the horizon is shown in Fig.1 (left panel) of the main text. The figure shows the contour lines which, as explained above, coincide with the flow lines of the current J^μ .

As seen in Fig.1, flow lines form loops (blue online). A loop of current generates a magnetic field in the orthogonal direction, hence the loops in Fig.1 encircle (pieces of) radially directed vortices approximately described by (9.21). The special feature of these EW vortices is that their magnetic field is enhanced by the condensate: it vanishes at the vortex center where the condensate is zero and maximal where the condensate is maximal [22, 23]. In other words, these vortices resemble hollow tubes: everything is concentrated at the tube surface and nothing is inside.

There are 4 vortices on the visible side of the surface in Fig.1 and the same number on the other side, so that altogether there are $8 = n - 2$ vortices homogeneously distributed over the horizon. The total magnetic flux is $2\pi \times n$, and the difference $|n| - 2$ arises because for $n = 2$ the black hole is spherically symmetric [16] hence there are no vortices at all. We checked that minimization of (9.28) gives one vortex for $n = 3$, two vortices for $n = 4$, etc. These solutions correspond to the global energy minimum.

The axially symmetric configuration with $c_m \propto \delta_{m0}$ is also a stationary point of the energy (9.28), which can be viewed as a system in which all elementary vortices merge into two oppositely directed collective multi-vortices generated by two oppositely-directed azimuthal currents.

The Hessian matrix has negative eigenvalues in this case, therefore such solutions are unstable and decay into non-axially symmetric ones. The exceptional case is $|n| = 2$ when only $m = 0$ is possible; the corresponding solution is stable in the flat space limit [32], while its gravitating version should very likely to be stable too. Another exceptional case is $|n| = 4$ when the values of $c_0, c_{\pm 1}$ corresponding to the global energy minimum can be transformed to $c_m \propto \delta_{m0}$ by a global rotation. Therefore, the axially symmetric configuration is already in the global energy minimum.